J. Am. Soc. Mass Spectrom. (2016) 27:1491–1498
DOI: 10.1007/s13361-016-1424-y

RESEARCH ARTICLE

Formation of Metal-Related Ions in Matrix-Assisted Laser Desorption Ionization

Chuping Lee,[1,2] I-Chung Lu,[1] Hsu Chen Hsu,[1] Hou-Yu Lin,[1,2] Sheng-Ping Liang,[1] Yuan-Tseh Lee,[1,2] Chi-Kung Ni[1,3]

[1]Institute of Atomic and Molecular Sciences, Academia Sinica, Taipei, 10617, Taiwan
[2]Department of Chemistry, National Taiwan University, Taipei, 10617, Taiwan
[3]Department of Chemistry, National Tsing Hua University, Hsinchu, 30013, Taiwan

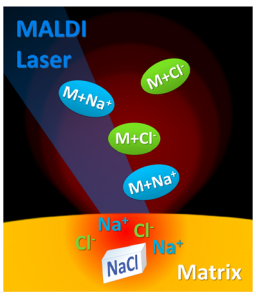

Abstract. In a study of the metal-related ion generation mechanism in matrix-assisted laser desorption ionization (MALDI), crystals of matrix used in MALDI were grown from matrix- and salt-containing solutions. The intensities of metal ion and metal adducts of the matrix ion obtained from unwashed crystals were higher than those from crystals washed with deionized water, indicating that metal ions and metal adducts of the matrix ions are mainly generated from the surface of crystals. The contributions of preformed metal ions and metal adducts of the matrix ions inside the matrix crystals were minor. Metal adducts of the matrix and analyte ion intensities generated from a mixture of dried matrix, salt, and analyte powders were similar to or higher than those generated from the powder of dried droplet crystals, indicating that the contributions of the preformed metal adducts of the matrix and analyte ions were insignificant. Correlation between metal-related ion intensity fluctuation and protonated ion intensity fluctuation was observed, indicating that the generation mechanism of the metal-related ions is similar to that of the protonated ions. Because the thermally induced proton transfer model effectively describes the generation of the protonated ions, we suggest that metal-related ions are mainly generated from the salt dissolution in the matrix melted by the laser.

Keywords: MALDI, Ionization mechanism, Metal ion, Thermally induced dissolution, Thermal model

Received: 16 November 2015/Revised: 17 May 2016/Accepted: 20 May 2016/Published Online: 15 June 2016

Introduction

The ions of peptides and proteins are generated in matrix-assisted laser desorption ionization (MALDI) as protonated peptides and protonated proteins, respectively. Many studies on MALDI have discussed the procedures involved in generating these protonated peptides and proteins [1–15]. Carbohydrate ions are generated in MALDI as sodiated or potassiated carbohydrates. According to Spengler et al., the appearance of Na^+ in mass spectra indicates the onset of a collective volume process in desorption [16]. The cationization in the gas phase of a neutral analyte formed under MALDI conditions has been investigated [17, 18]. This study demonstrated that the ion intensity of sodiated peptides can be enhanced through the beam of neutral analyte formed in MALD intercepted by a beam of sodium cation. Liao and Allison suggested three possible mechanisms for generating sodiated analyte ions in MALDI: excited-state salt chemistry, protonation of the analyte sodium salt, and gas-phase capture of Na^+ by the analyte [19]. In the mechanisms of excited-state salt chemistry and protonation of the analyte sodium salt, the sodium salts of the matrix and analyte must be generated (preformed) before laser irradiation. Karas and colleagues proposed the lucky survivor model for describing metal ion generation [3, 4]. According to this model, ions, including metaliated and protonated ions, were produced (preformed) in solution during sample preparation. However, only some of the ions were neutralized during crystallization. The rest of the ions remained as ions (preformed ions) in crystals. Laser desorption converted these ions from a solid state into a gas phase.

Recently, we proposed a thermal proton transfer model to describe the generation of protonated ions in MALDI [10–15]. The absorption of laser light by matrix molecules results in an increased temperature, and the solid matrix melts and behaves in a similar manner to a polar solvent before the occurrence of desorption. Ions are generated by thermally induced reactions in a polar-solvent-like matrix. Proton transfer is the reaction in which the heat of reaction is lowest for the generation of ions.

Correspondence to: Chi–Kung Ni; *e-mail:* ckni@po.iams.sinica.edu.tw

Proton transfer can be considerably enhanced at high temperatures. Studies have demonstrated [10–15] that the amount of protonated ions generated by a thermally induced proton transfer reaction has an order of magnitude similar to that observed in experimental measurements.

In this study, we performed three separate experiments to measure the contributions of the preformed metal and metal adducts of the matrix and analyte ions in MALDI, and we evaluated the correlation between these metal-related ions and protonated ions. The first experiment demonstrated that the metal and metal adducts of the matrix ions observed in MALDI were not generated from the metal-related preformed ions inside the matrix crystals. The second experiment revealed that metal adducts of the matrix and analyte ions are not mainly produced from the preformed ions. The third experiment demonstrated that the ion intensity fluctuations in the metal-related ions correlated with those in the protonated ions, indicating that both metal-related ions and protonated ions are produced through the same ionization mechanism. Finally, we adopted the concept of the thermal proton transfer model [10–15] for describing the generation of metal-related ions through the thermally induced dissolution of salts.

Experimental

Washed and Unwashed Single Crystals

Single crystals grown from the following solutions were used for MALDI. The molar ratios of LiCl (or NaCl) and 2,5-dihydroxybenzoic acid (2,5-DHB, 99%, purchased from Acros Organics, Geel, Belgium) in six solutions were 0:1, 1×10^{-5}:1, 1×10^{-4}:1, 1×10^{-3}:1, 1×10^{-2}:1, and 5×10^{-2}:1. The solvents were methanol and water in a 3:1 ratio. Several crystals were grown from each solution. Two crystals of similar size (approximately $3 \times 1 \times 0.5$ mm measured using a caliper) were selected from each solution. One crystal was used directly without further processing. The other crystal was washed three times with deionized water before use. In each washing process, the crystal was immersed in fresh deionized water for approximately 45 s. The sizes of the crystals did not change considerably after washing.

A commercial time-of-flight (TOF) mass spectrometer (Autoflex III; Bruker Daltonik GmbH, Bremen, Germany) was used for MALDI mass spectra measurements. To reduce systemic errors, 12 crystals (two crystals for each concentration, one washed and the other unwashed) were analyzed on the same day. Mass spectra were obtained for the washed (with deionized water) and unwashed crystals alternately. The entire experiment, including crystal preparation and mass spectra measurements, were repeated three times.

Mixture of Dried Powder Versus Dried Droplet Crystal Powder

Two groups of samples were prepared in this experiment. For the first group of samples, dried powders of the matrix 2,5-DHB, analyte, and salt (LiCl or NaCl) were mixed without a solvent. Water contamination in the matrix crystals was removed by placing the crystals in a vacuum chamber at room temperature for more than 12 h before use. The pressure of the vacuum chamber, which was pumped by an Edwards XDS-10 oil-free dry scroll vacuum pump (Crawley, UK), was $<10^{-1}$ Torr. LiCl or NaCl crystals were baked in a vacuum oven (Tokyo Rikakikai Co., Ltd., Japan, EYELA, model: VOS-201SD1SD, 373 K, 10^{-1} Torr) for 12 h. The vacuum oven was pumped by another Edwards XDS-10 oil-free dry scroll vacuum pump. The baking and pumping chambers ensure that samples contain minimal water on the surface. The vacuum chamber and oven were then vented to atmospheric pressure by using dry N_2 gas, and these crystals were sealed in air-tight containers in the oven or vacuum chamber before being transferred into a dry box. The matrix, analyte, and salt crystals in a molar ratio of 100:0.5 (for sucrose and maltopentaose, or 0.05 for pullulan):1 were mixed and hand-ground for 10 min. A small portion of the powdered mixture was separated and further ground for 20 min. The powders were then pressed using a stainless steel rod to form thin disks (approximately 0.5–1 mm thick). The disks were placed in the holes (0.5 mm deep and 2 mm in diameter) of a modified sample plate (prespotted Anchor Chip PAC 96 HCCA; Bruker Daltonik, GmbH). The samples and sample plate were sealed in a container purged with dry N_2 gas before they were removed from the dry box. Finally, they were placed in a mass spectrometer for conducting mass spectra measurements. A small amount of salt and matrix powders was used to measure the size of powder particles through optical microscopy. The sizes of both the salt and matrix powder particles depend on the grinding time. The sizes of particles ground for 10 min ranged from several micrometers to several tens of micrometers. However, the sizes of the particles ground for 30 min decreased.

For preparing the second group of samples, the crystals of vacuum-dried droplets were hand-ground into fine powder for 10 min. The molar ratio of the matrix, analyte, and salt in the solution (75% aqueous acetonitrile) of the droplets was 100 (matrix):0.5 (for sucrose and maltopentaose, or 0.05 for pullulan):1 (salt). The powder was pressed to form thin disks and placed in the holes of the sample plate as described.

A modified commercial MALDI-TOF (Autoflex III; Bruker Daltonik GmbH, Bremen, Germany) mass spectrometer was used for ion detection. The load-lock chamber was purged with dry N_2 gas, and the gap between the sample entrances of the spectrometer and vacuum chamber, which was initially exposed to air, was sealed and purged with dry N_2 gas. To reduce systemic errors, five samples belonging to each group were placed on the same sample plate and measured alternately on the same day. The entire experiment was repeated five times for LiCl and three times for NaCl.

The desorbed neutral molecules were measured using a modified crossed-molecular beam machine. It included a load-lock chamber, a main chamber, and a detection chamber. The details have been given elsewhere [20, 21]. Only a brief description is given here. A stainless steel cylindrical sample

holder was positioned inside the main chamber where the pressure was less than 1×10^{-7} Torr. The laser irradiation spot on the sample surface was located at the reaction center of the main chamber. Upon laser irradiation, the desorbed neutral molecules flew into the detection chamber and were detected by a mass spectrometer. The mass spectrometer consisted of an electron-impact ionizer located at 350 mm from the laser irradiation spot on the solid sample surface, a quadrupole mass spectrometer, and a Daly ion detector. Neutrals that flew into detection chamber were ionized by an electron-impact ionizer. In this work, we turned off the DC voltage of the quadrupole mass spectrometer. It allowed all the ionized neutrals to be guided by the quadrupole and eventually detected by the ion detector. The velocity distribution was obtained from the different arrival times of desorbed neutrals at detector.

Correlation Between Intensity Fluctuations in Metal and Metal Adducts of the Matrix Ions and Protonated Ions

The third experiment entailed investigating typical dried droplet samples of 2,5-DHB by using a home-made time-of-flight (TOF) mass spectrometer and a laser beam from the third harmonic of a Nd:YAG laser (355 nm, 5-ns pulse duration, Minlite II, Continuum). The laser beam was split into two parts by using a beam splitter. One part entered the TOF mass spectrometer for the MALDI experiment. The other part was used to measure the energy of each laser pulse by employing an energy meter. The outputs of the TOF mass spectrometer and energy meter were recorded using an oscilloscope for each laser shot.

Results and Discussion

Washed and Unwashed Single Crystals

Figure 1 shows the ion intensities of Li^+-related ions obtained from the mass spectra of the washed (with deionized water) and unwashed crystals. These cations included Li^+, $(2,5\text{-DHB+Li})^+$, $(2,5\text{-DHB-H+2Li})^+$, $((2,5\text{-DHB})_2\text{+Li})^+$, and $((2,5\text{-DHB})_3\text{-3H+4Li})^+$. Each data point in Figure 1 represents an average of 600 laser shots, which include the measurement of 3 crystals, 10 positions from each crystal, and 20 laser shots at each position. As illustrated in this figure, the Li^+-related ion intensities for the unwashed crystals strongly correlated with the initial LiCl concentration in the solution. Specifically, the Li^+-related ion intensities increased with the initial LiCl concentration in the solution. By contrast, for the crystals washed with deionized water, the Li^+-related ion intensities did not change with the initial LiCl concentration in the solution. These results suggest that the amount of Li^+-related compounds present within the matrix crystal because of crystal defects was low. Li^+-related materials mainly existed on the crystal surface, and these materials could be easily removed using deionized water. Because the 2,5-DHB crystals were grown from the LiCl-containing solution, one possible Li^+-related material is a layer

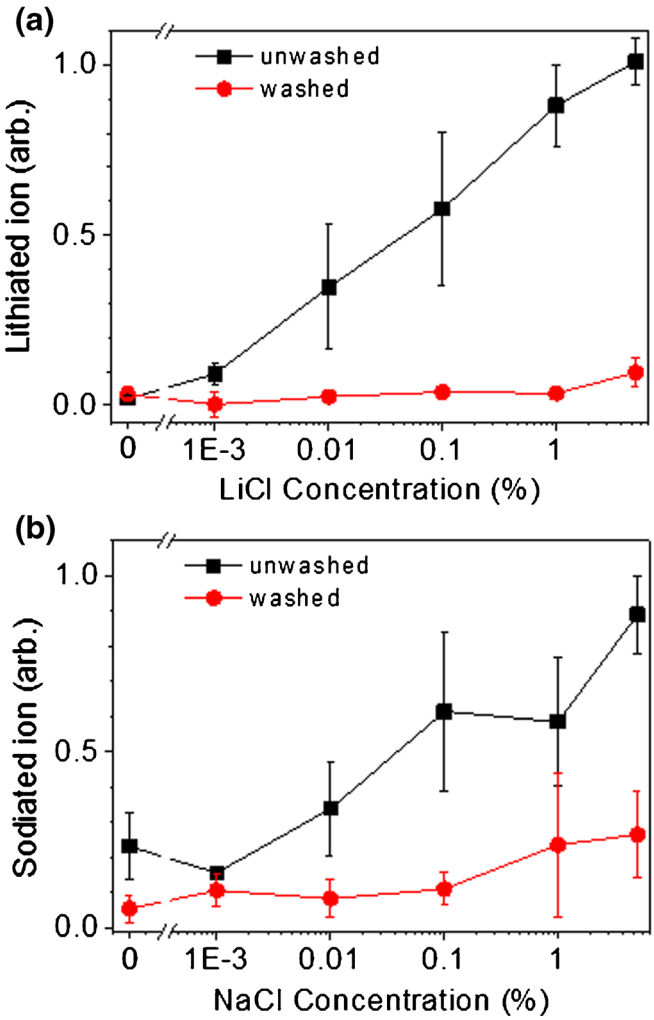

Figure 1. **(a)** MALDI Li^+-related ion intensities of the crystals grown from a LiCl-containing 2,5-DHB solution at different concentrations. **(b)** MALDI Na^+-related ion intensities of the crystals grown from a NaCl-containing 2,5-DHB solution at different concentrations. These Li^+- or Na^+-related ions include metal ions and metal adducts of the matrix. Red diamonds represent the ion intensities of the deionized water-washed crystals, and black squares represent the ion intensities of the unwashed crystals. The scale of the X axis is linear before the break and logarithmic after the break. High ion intensity differences between crystals indicate that most of the Li^+- and Na^+-related ions do not exist inside matrix crystals. *P*-values for the LiCl and NaCl samples are 0.00036 and 0.019, respectively, indicating the ion intensity difference between water-washed crystals and unwashed crystals

of small LiCl crystals or lithium salt of matrix on the surface. The small LiCl crystals or lithium salt of matrix were grown from the small droplets of the solution attached to the surface of the 2,5-DHB crystals when these crystals were taken from the solution, followed by solvent vaporization.

Similar results were obtained for the crystals grown in the NaCl-containing solution, as illustrated in Figure 1b. Although the difference in Na^+-related ion intensities between the crystals was not as high as that in Li^+-related ion intensities, the

results still indicated that most of the Na^+-related ions were mainly obtained from NaCl or sodium salt of matrix existing on the crystal surface. The smaller difference between the two types of crystals and high fluctuation in intensity in Figure 1b may be attributed to the Na^+ background in the deionized water.

Mixture of Dried Powder Versus Dried Droplet Crystal Powder

Figure 2a and b show the intensities of lithiated matrix ions and lithiated sucrose ions generated from the mixture of dried 2,5-DHB, 0.5% sucrose, and 1% LiCl powders and from the powder of dried droplets whose solution contained 2,5-DHB, 0.5% sucrose, and 1% LiCl. Each data point represents the accumulation of 1000 laser shots, including 10 spots from each sample, 20 laser shots at each sample spot, and five samples. The ion intensities of the dried powder mixture (DPM) were similar to that of dried droplet powder (DDP). Figure 2c shows the intensities of lithiated maltopentaose ions generated from the mixture of dried 2,5-DHB, 0.5% maltopentaose, and 1% LiCl powders and from the powder of dried droplets whose solution contained 2,5-DHB, 0.5% maltopentaose, and 1% LiCl. The ion intensities of DDP were higher than those of DPM when the grinding period of the DPM was 10 min. However, when we increased the grinding period of the DPM to 30 min, the ion intensities of the DPM were close to those of the DDP.

Karas et al. proposed that ions were preformed in solution during sample preparation [3, 4]. The dried droplet crystal powder can produce preformed Li^+ ions and Li^+ adducts of the matrix and analyte ions in the crystals during sample preparation. By contrast, the preparation of the dried 2,5-DHB, sucrose (or maltopentaose), and LiCl powder mixture involved no solvent; the samples containing this mixture have a low probability of producing preformed ions. Preformed ions may be produced in DPM as follows. The long grinding period engenders two effects: one effect is the small particle size of the powder and uniformity of the mixed powder, and the other effect is the local high temperature. If the local temperature reaches the melting point of the matrix during grinding, the local melting of the matrix can cause the dissolution of salt and produce preformed ions. In this experiment, all the samples were hand-ground at room temperature, and the grinding speed was slow. Although the temperature of a small fraction of the sample may exceed room temperature during grinding, it was unlikely that every part of the sample reached the melting point of 2,5-DHB (200 °C) sooner or later during grinding. Therefore, the similar ion intensities of the DDP and DPM ground for 30 min cannot be completely attributed to the local matrix melting.

Figure 3a illustrates the Na^+-related ions generated from the mixture of dried 2,5-DHB, 0.5% maltopentaose, and 1% NaCl powders and from the powder of dried droplet crystals whose solution involved 2,5-DHB, 0.5% maltopentaose, and 1% NaCl. Because a small amount of Na^+ ions was always present

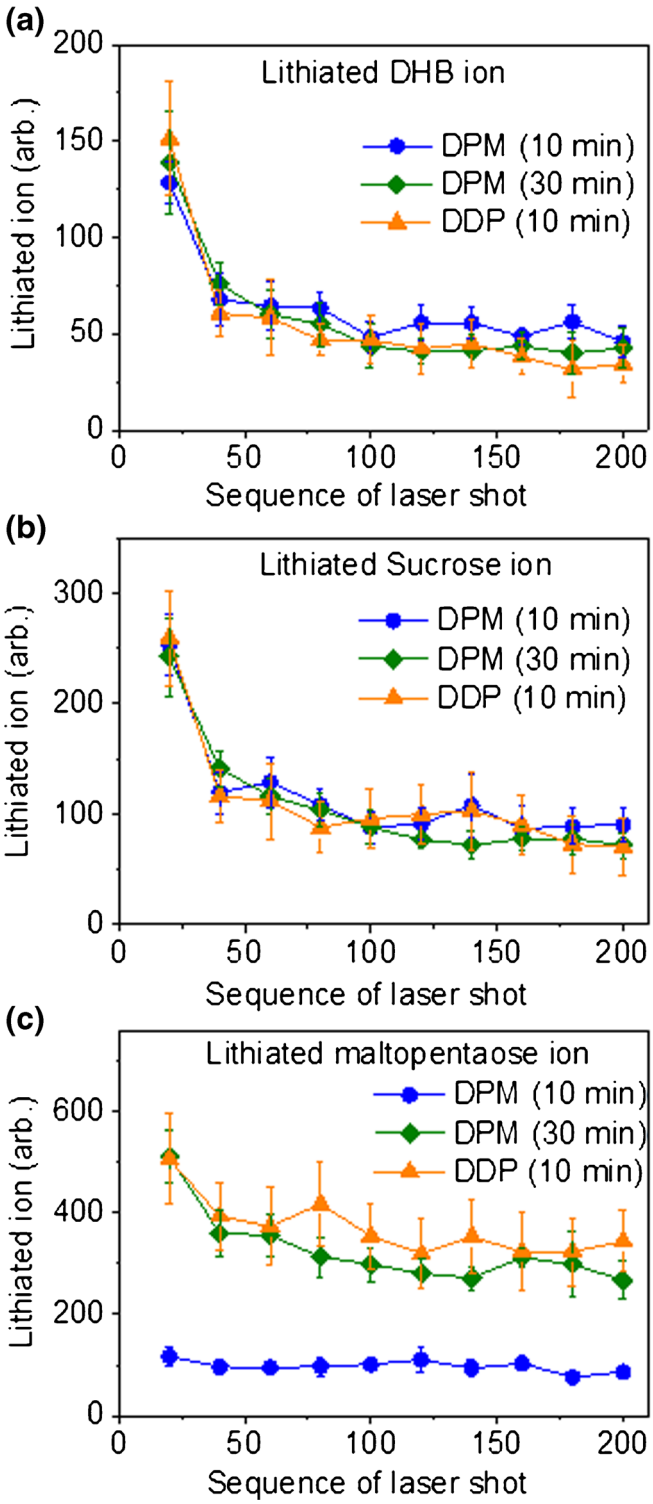

Figure 2. Lithiated ion intensities from three samples: dried droplet powder (DDP, orange triangles) ground for 10 min, dried powder mixture (DPM) ground for 10 min (blue circles), and DPM ground for 30 min (olive diamonds). The molar ratio of the matrix 2,5-DHB, analyte (sucrose), and salt (LiCl) in **(a)** and **(b)** is 100:0.5:1, and the molar ratio of the matrix 2,5-DHB, analyte (maltopentaose), and salt (LiCl) in **(c)** is 100:0.5:1. The *P*-values for DDP and DPM ground for 30 min are **(a)** 0.67, **(b)** 0.67, **(c)** 0.95, indicating no difference of ion intensities between DDP and DPM ground for 30 min

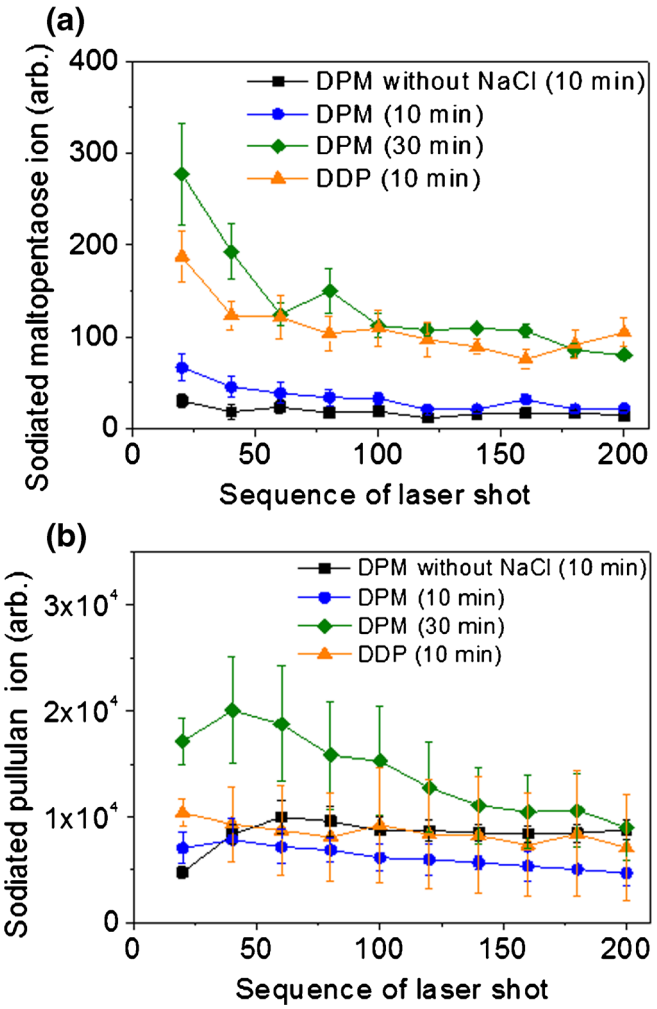

Figure 3. Sodiated ion intensity of **(a)** maltopentaose and **(b)** pullulan (6k) from four samples: (1) DDP (orange triangles) ground for 10 min, and the matrix 2,5-DHB, analyte (maltopentaose or pullulan), and salt (NaCl) are present in a molar ratio of 100:0.5 (for maltopentaose or 0.05% for pullulan):1; (2) DPM without 1% NaCl ground for 10 min (black squares), and the matrix 2,5-DHB, analyte (maltopentaose or pullulan), and salt (NaCl) are present in a molar ratio of 100:0.5 (for maltopentaose, or 0.05% for pullulan):0; (3) DPM ground for 10 min (blue circles); and (4) DPM ground for 30 min (olive diamonds), and the molar ratios of the powder mixture in samples (3) and (4) are the same as those in sample (1)

in the matrix or analyte samples, the Na^+ ion background, measured using the DPM of 2,5-DHB and 0.5% maltopentaose, is shown in Figure 3a for comparison. Figure 3a indicates that the intensities of the sodiated maltopentaose ions generated from the DPM are higher than those of the sodiated maltopentaose ions generated from the powder of the dried droplets. Similar phenomena were observed for analyte pullulan (6k), as illustrated in Figure 3b.

If the process of generating preformed ions at a local high temperature due to long grinding periods is a major sodiated ion generation mechanism, the intensities of the sodiated ions generated from the DPM are at most as high as those of the sodiated ions generated from the DDP. However, both Figure 3a and b show that the intensities of the sodiated ions generated from the DPM with a long grinding period are higher than those of the sodiated ions generated from the DDP, indicating that the size of the powder and uniformity of the mixed powder are more crucial than the preformed ions.

Another comparison of dried droplet powder and dried powder mixture is the value of ion-to-neutral ratio (so-called ion generation efficiency or ion yield) from each sample. The ion-to-neutral ratio is defined as the ratio of the desorbed ions to the desorbed neutrals. Ion-to neutral ratio is a commonly used parameter in theoretical models to determine ionization mechanism. It avoids the bias of different desorption capability in the comparison of different samples (different sample preparation methods, or different matrices, etc.) The desorbed neutrals are illustrated in Figure 4. The measurements show that the desorbed neutrals from dried droplet powder and dried powder mixture are similar in quantity and in velocity distributions. Ion-to-neutral ratios, obtained from combining the relative ion intensities and desorbed neutrals, suggest that a sample without the preformed ions (dried power mixture) can generate Li^+-related ions as efficiently as a sample with preformed ions (dried droplet powder), or a sample without the preformed ions is more efficient to generate Na^+-related ions than a sample with preformed ions.

Correlation Between Intensity Fluctuations in Metal and Metal Adducts of the Matrix Ions and Protonated Ions

In the previous two experiments, high molar ratios of salt (LiCl or NaCl) were used in the samples. The concentration of metal and metal adducts of the matrix ions may exceed the capacity of the matrix crystal defects. As such, the "extra" salt does *not* produce preformed ions. Typical dried droplet samples were used in the third experiment. The solution of the droplets contained 2,5-DHB in water and acetonitrile in a 1:3 ratio. Two sample types were investigated in the experiment. In the first sample type, no salt was added to the solution. Like most MALDI experiments, sodiated ions were still observed in the mass spectra. Na^+ may come from impurities in 2,5-DHB or solvents or from glassware contaminations during sample preparation.

Figure 5a shows the intensities of the Na^+-related ions (Na^+ and Na^+ adducts of the matrix) and protonated ions as a function of the sequence of laser shots from the same sample spot. Both the Na^+-related ion and protonated ion intensities fluctuated from shot to shot. No clear change (increase or decrease) in the ion intensity as a function of the laser sequence was observed. Although the amplitudes of these two fluctuations are not always the same, this figure indicates a correlation between the intensities of the Na^+-related ions and protonated ions. A more efficient method of revealing the correlation is to plot the Na^+-related ion intensity as a function of the protonated ion intensity for each laser shot, as illustrated in Figure 5b,

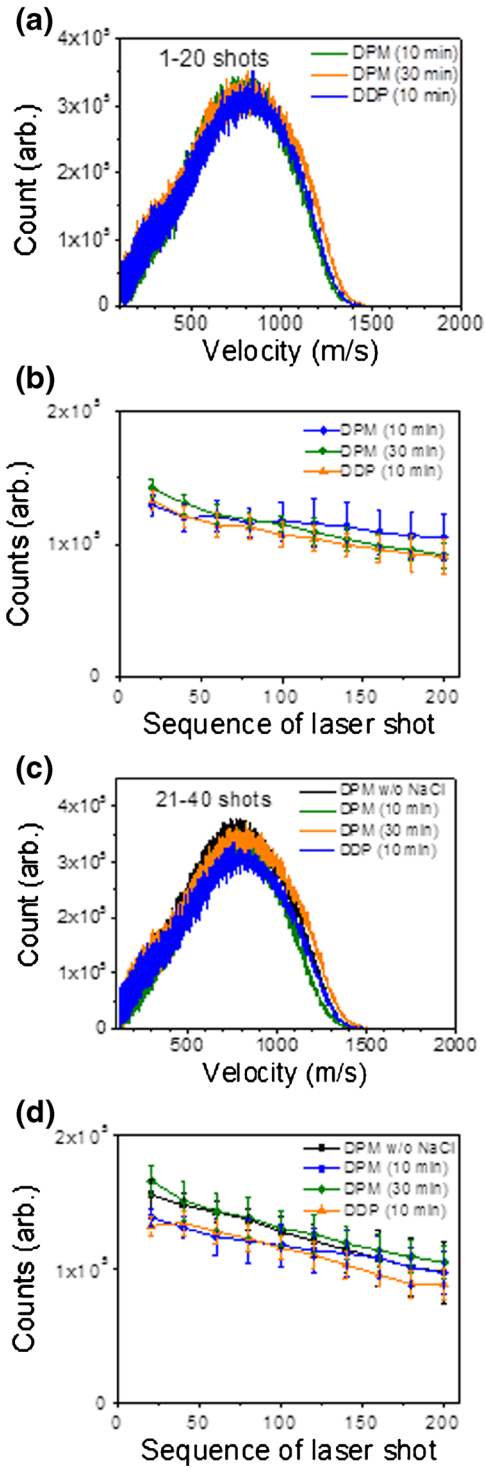

Figure 4. **(a)** and **(c)**: velocity distributions of desorbed neutrals from various samples. **(b)** and **(d)**: desorbed neutrals as a function the sequence of laser shot for various samples. Samples in **(a)** and **(b)** are dried droplet powder (DDP) ground for 10 min, dried powder mixture (DPM) ground for 10 min, and DPM ground for 30 min. The molar ratio of the matrix 2,5-DHB, analyte (sucrose), and salt (LiCl) is 100:0.5:1. Samples in **(c)** and **(d)** are DDP ground for 10 min, DPM ground for 10 min, DPM ground for 30 min. The molar ratio of the matrix 2,5-DHB, analyte (maltopentaose), and salt (NaCl) is 100:0.5:1, except the sample (DPM w/o NaCl), in which no NaCl was added in sample

which shows that the increase in the Na^+-related ion intensity is approximately proportional to the increase in the protonated ion intensity.

The laser energy fluctuation in this experiment was approximately 10%–15%. To ensure that the laser energy increase (due to laser energy fluctuation) did not engender the increases in both the Na^+-related ions and protonated ion intensities, we measured the laser pulse energy for each laser shot and divided the laser energy into five regions. Figure 5b indicates that the increase in the Na^+-related ion intensity remains proportional to the increase in the protonated ion intensity for each laser energy region. If the increase in both the Na^+-related ion and protonated ion intensities resulted from the laser energy increase, signals for the lowest energy should have been distributed in the lower-left corner of Figure 5b, and those for the highest energy should have been distributed in the upper-right corner of this figure. However, the signals from different laser energy regions overlapped, indicating that a factor different from the laser energy causes the fluctuation in Na^+-related ion and protonated ion intensities simultaneously. This factor is related to the ion generation efficiencies of both the Na^+-related ion and protonated ions.

In the second sample type, the droplet solution involved 2,5-DHB and 1% NaCl. Figure 5c illustrates the fluctuations in the Na^+-related ion and protonated ion intensities as a function of the sequence of laser shots from the same sample spot. Figure 5d clearly shows the correlation between the fluctuations in the Na^+-related ion and protonated matrix ion intensities. The results suggest that the sodiated ion generation mechanisms for both low and high concentrations of NaCl are related to the protonated ion generation mechanism.

Thermally Induced Dissolution of Salts

The preceding results suggest that the preformed ions did not contribute to the major ionization mechanism of the metal-related ions in MALDI, and the ion generation efficiencies of the metal-related ions and protonated ions were influenced by a similar mechanism. One possibility is that both metal and protonated ions are produced through the same ion generation mechanism.

We have recently proposed a thermal proton transfer model to describe the procedures involved in generating protonated ions in MALDI [10–15]. In this model, a high surface temperature is engendered by the absorption of laser light by matrix molecules. The solid matrix melts and behaves in a similar manner to a polar solvent before the occurrence of desorption. Protons are generated through thermally induced proton transfer reactions in a polar-solvent-like matrix. Here, we adopted a similar concept and propose that metal ions are generated through the thermally induced dissolution of salts,

$$MCl_{(s)} \rightarrow M^+_{(sol)} + Cl^-_{(sol)} (M^+ = Li^+, Na^+) \quad (1)$$

where the subscripts *s* and *sol*, respectively, represent the solid phase and solution in which the matrix is the solvent and salt is the solute. Metal adducts of the matrix and analyte ions can be

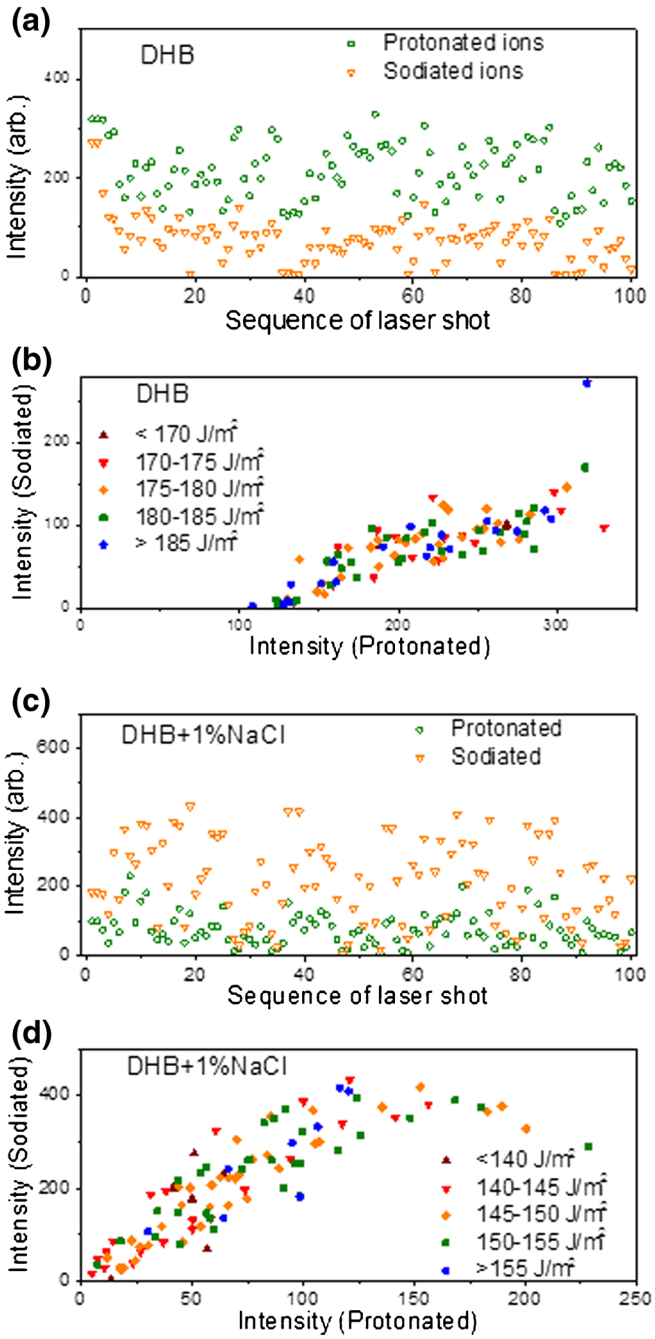

Figure 5. **(a)** and **(c)**: Sodiated and protonated ions as a function of the sequence of laser shots from the same spot of the sample. Shot-to-shot ion intensity fluctuations are observed in both sodiated and protonated ions. Data in **(a)** and **(c)** are replotted in **(b)** and **(d)**, respectively. Shot-to-shot laser energy fluctuation is approximately 15%. The data points in **(b)** and **(d)** are divided into five groups, with each group representing a small region of laser energy; data from the different laser energy regions in **(b)** and **(d)** overlap, indicating that the increase in the sodiated and protonated ion intensities is not engendered by the increase (fluctuation) in laser energy. Strong correlation between the sodiated and protonated ions suggests that they are generated from a related ionization mechanism

produced when metal ions attach to the matrix and analyte molecules during the desorption process.

Although metal ions can be generated by the thermally induced dissolution of salts in MALDI, the metal ion intensity strongly depends on the homogeneity of the salt crystals distributed in the matrix and degree of contact between the salt and the matrix crystals. In a thermally induced proton transfer reaction in a pure matrix, matrix molecules act as both the solvent and solute. Therefore, the solute is homogeneously distributed in the solvent, and the thermally induced proton transfer reaction can reach equilibrium easily. By contrast, salt molecules are not homogeneously distributed among matrix molecules. Salt molecules form small crystals, and only the molecules on the crystal surface establish a favorable contact with the matrix molecules. Because the high-temperature polar-solvent-like matrix exists for only a short period (<100 ns) [22], and because the amount of this matrix is small (desorbed matrix thickness is <100 nm[15]), salt crystals measuring several micrometers in size are unlikely to be completely dissolved; therefore, the thermally induced dissolution of the salt crystal cannot reach equilibrium during MALDI. The nonequilibrium of Reaction 1 renders the intensities of metal ions lower than those of protonated ions.

Our results suggest that close contact between salt and matrix molecules increases the probability of the reaction generating metal-related ions. A similar concept can be applied to an analyte and matrix. Close contact between analyte and matrix molecules also increases the analyte ion generation efficiency. Moreover, converting analyte molecules into the gas phase during sublimation is beneficial. A study revealed that the performance of MALDI was inversely proportional to the crystal size, suggesting the importance of close contact between analyte and matrix molecules [23]. We suggest that the success of many solvent-free MALDI experiments in previous studies [23–34] indicate that the contribution of preformed ions is inconsequential. These results are consistent with those of our proposed mechanism.

Conclusion

First, we demonstrated that Li^+ and Na^+-related ions are not mainly generated by preformed ions in 2,5-DHB. The shot-to-shot fluctuation in Na^+-related ions is strongly correlated to that in protonated ions. The results suggest that the thermally induced dissolution of salts in MALDI is the major ion generation mechanism. Second, because of the inhomogeneous distribution of salt crystals in the matrix, the thermally induced dissolution of salts did not reach equilibrium, and the intensity of the metal ions was strongly affected by the degree of contact between the salt and matrix crystals. Third, because the generation of preformed metal-related ions within matrix crystals depends on the solid-state structure of the matrix, size and charge of metal ions, and interaction between the metal ions and matrix molecules, we did not exclude the possible contribution of preformed ions for other metal ions and matrices.

Forth, the experimental observation reported in this work supports the ionization mechanism we proposed. It does not support the current preformed ion model. However, it does not exclude the possibility of the other models, for example, a completely new model proposed in the future, or the modification of the current preformed ion model.

Both the thermally induced proton transfer model proposed in our previous studies [10–15] for generating protonated ions in MALDI and the model of thermally induced dissolution of salt proposed in the current study for generating metal-related ions in MALDI can be combined and simplified as a thermal model, which suggests that thermally induced reactions are crucial for ion generation in MALDI.

Acknowledgments

The authors acknowledge support of the Thematic Research Program, Academia Sinica, Taiwan (AS-102-TP-A08) and National Science Council, Taiwan (NSC 100-2113-M-001-026-MY3).

References

1. Ehring, H., Karas, M., Hillenkamp, F.: Role of photoionization and photochemistry in ionization progress of organic-molecules and relevance for matrix-assisted laser desorption ionization mass spectrometry. Org. Mass Spectrom. **27**, 472–480 (1992)
2. Knochenmuss, R.: A quantitative model of ultraviolet matrix-assisted laser desorption/ionization. J. Mass Spectrom. **37**, 867–877 (2002)
3. Karas, M., Glückmann, M., Schäfer, J.: Ionization in matrix-assisted laser desorption/ionization: singly charged molecular ions are the lucky survivors. J. Mass Spectrom. **35**, 1–12 (2000)
4. Karas, M., Kruger, R.: Ion formation in MALDI: The cluster ionization mechansim. Chem. Rev. **103**, 427–439 (2003)
5. Allwood, D.A., Dyer, P.E., Dreyfus, R.W., Perera, I.K.: Plasma modeling of matrix assisted UV laser desorption ionisation (MALDI). Appl. Surf. Sci. **109/110**, 616–620 (1997)
6. Allwood, D.A., Dyer, P.E., Dreyfus, R.W.: Ionization modeling of matrix molecules in ultraviolet matrix-assisted laser desorption/ionization. Rapid Commun. Mass Spectrom. **11**, 499–503 (1997)
7. Niu, S.F., Zhang, W.Z., Chait, B.T.: Direct comparison of infrared and ultraviolet wavelength matrix-assisted laser desorption/ionization mass spectrometry of proteins. J. Am. Soc. Mass Spectrom. **9**, 1–7 (1998)
8. Chen, X., Carroll, J.A., Beavis, R.C.: Near-ultraviolet-induced matrix-assisted laser desorption/ionization as a function of wavelength. J. Am. Soc. Mass Spectrom. **9**, 885–891 (1998)
9. Lai, Y.H., Wang, C.C., Lin, S.H., Lee, Y.T., Wang, Y.S.: Solid-phase thermodynamic interpretation of ion desorption in matrix-assisted laser desorption/ionization. J. Phys. Chem. B **114**, 13847–13852 (2010)
10. Chu, K.Y., Lee, S., Tsai, M.T., Lu, I.C., Dyakov, Y.A., Lai, Y.H., Lee, Y.T., Ni, C.K.: Thermal proton transfer reactions in ultraviolet matrix-assisted laser desorption/ionization. J. Am. Soc. Mass Spectrom. **25**, 310–318 (2014)
11. Chu, K.Y., Lee, S., Tsai, M.T., Lu, I.C., Dyakov, Y.A., Lai, Y.H., Lee, Y.T., Ni, C.K.: Erratum to: Thermal proton transfer reactions in ultraviolet matrix-assisted laser desorption/ionization. J. Am. Soc. Mass Spectrom. **25**, 1087 (2014)
12. Lu, I.C., Lee, C., Chen, H.Y., Lin, H.Y., Hung, S.W., Dyakov, Y.A., Hsu, K.T., Liao, C.Y., Lee, Y.Y., Tseng, C.M., Lee, Y.T., Ni, C.K.: Ion intensity and thermal proton transfer in ultraviolet matrix-assisted laser desorption/ionization. J. Phys. Chem. B **118**, 4132–4139 (2014)
13. Lu, I.C., Chu, K.Y., Lin, C.Y., Wu, S.Y., Dyakov, Y.A., Chen, J.L., Gray-Weale, A., Lee, Y.T., Ni, C.K.: Ion-to-neutral ratios and thermal proton transfer in matrix-assisted laser desorption/ionization. J. Am. Soc. Mass Spectrom. **26**, 1242–1251 (2015)
14. Gray-Weale, A., Ni, C.K.: Comment on: "Energetics and kinetics of thermal ionization models of MALDI" by Richard Knochenmuss. J. Am. Soc. Mass Spectrom. **26**, 2162–2166 (2015)
15. Lu, I.C., Lee, C., Lee, Y.T., Ni, C.K.: Ionization mechanism of matrix-assisted laser desorption/ionization. Ann. Rev. Anal. Chem. **8**, 21–39 (2015)
16. Spengler, B., Karas, M., Bahr, U., Hillenkamp, F.: Excimer laser desorption mass spectrometry of biomolecules at 248 and 193 nm. J. Phys. Chem. **91**, 6502–6506 (1987)
17. Wang, B.H., Dreisewerd, K., Bahr, U., Karas, M., Hillenkamp, F.: Gas-phase cationization and protonation of neutrals generated by matrix-assisted laser desorption. J. Am. Soc. Mass Spectrom. **4**, 393–398 (1993)
18. Belov, M.E., Myatt, C.P., Derrick, P.: Chemical ionization of neutral peptides produced by matrix-assistend laser desorption. Chem. Phys. Lett. **284**, 412–418 (1998)
19. Liao, P.C., Allison, J.: Ionization process in matrix-assisted laser desorption/ionization mass spectrometry: matrix-dependent formation of $[M + H]^+$ versus $[M + Na]^+$ ions of small peptides and some mechanistic comments. J. Mass Spectrom. **30**, 408–423 (1995)
20. Liang, C.W., Lee, C.H., Lin, Y.J., Lee, Y.T., Ni, C.K.: MALDI mechanism of dihydroxybenzoic acid isomers: desorption of neutral matrix and analyte. J. Phys. Chem. B **117**, 5058–5064 (2013)
21. Tsai, M.T., Lee, S., Lu, I.C., Chu, K.Y., Liang, C.W., Lee, C.H., Lee, Y.T., Ni, C.K.: Ion-to-neutral ratio of 2,5-dihydroxybenzoic acid in matrix-assisted laser desorption/ionization. Rapid Commun. Mass Spectrom. **27**, 955–963 (2013)
22. Koubenakis, A., Frankevich, V., Zhang, J., Zenobi, R.: Time-resolved surface temperature measurement of MALDI matrices under pulsed UV laser irradiation. J. Phys. Chem. A **108**, 2405–2410 (2004)
23. Trimpin, S., Räder, H.J., Müllen, K.: Investigations of theoretical principles for MALDI-MS derived from solvent-free sample preparation. Part I. Preorganization. Int. J. Mass Spectrom. **253**, 13–21 (2006)
24. Trimpin, S., Rouhanipour, A., Az, R., Räder, H.J., Müllen, K.: New aspects in matrix-assisted laser desorption/ionization time-of-flight mass spectrometry: a universal solvent-free sample preparation. Rapid Commun. Mass Spectrom. **15**, 1364–1373 (2001)
25. Trimpin, S., Grimsdale, A.C., Räder, H.J., Müllen, K.: Characterization of an insoluble poly(9,9-diphenyl-2,7-fluorene) by solvent-free sample preparation for MALDI-TOF mass spectrometry. Anal. Chem. **74**, 3777–3782 (2002)
26. Trimpin, S., Deinzer, M.L.: Solvent-free MALDI-MS for the analysis of biological samples via a mini-ball mill approach. J. Am. Mass Spectrom. **16**, 542 (2005)
27. Skelton, R., Dubois, F., Zenobi, R.: A MALDI sample preparation method suitable for insoluble polymers. Anal. Chem. **72**, 1707–1710 (2000)
28. Przybilla, L., Brand, J.D., Yoshimura, K., Räder, H.J., Müllen, K.: MALDI-TOF mass spectrometry of insoluble giant polycyclic aromatic hydrocarbons by a new method of sample preparation. Anal. Chem. **72**, 4591–4597 (2000)
29. Leuninger, J., Trimpin, S., Räder, H.J., Müllen, K.: Novel approach to ladder-type polymers: polydithiathianthrene via the intramolecular acid-induced cyclization of methylsulfinyl-substituted poly(meta-phenylene sulfide). Macromol. Chem. Phys. **202**, 2832–2842 (2001)
30. Wang, M.Z., Fitzgerald, M.C.: A solid sample preparation method that reduces signal suppression effects in the MALDI analysis of peptides. Anal. Chem. **73**, 625–631 (2001)
31. Dolan, A.R., Wood, T.D.: Analysis of polyaniline oligomers by laser desorption ionization and solventless MALDI. J. Am. Soc. Mass Spectrom. **15**, 893–899 (2004)
32. Hanton, S.D., Parees, D.M.: Extending the solvent-free MALDI sample preparation method. J. Am. Mass Spectrom. **16**, 90–93 (2005)
33. Trimpin, S., Spencer, P.S., Deinzer, M.L.: Evaluation of solvent-free MALDI-MS for the analysis of proteins via the mini-ball mill. Mol. Cell. Proteomics **4**, 311 (2005)
34. Trimpin, S., Keune, S., Räder, H.J., Müllen, K.: Solvent-free MALDI-MS: developmental improvements in the reliability and the potential of MALDI in the analysis of synthetic polymers and giant organic molecules. J. Am. Mass Spectrom. **17**, 661–671 (2006)